

Numerical study on performance of supersonic inlets with various three-dimensional bumps

Sang Dug Kim¹ and Dong Joo Song^{2,*}

¹*School of Automotive, Industrial and Mechanical Engineering, Daegu University, Korea*

²*School of Mechanical Engineering, Yeungnam University, Korea*

(Manuscript Received February 18, 2008; Revised May 1, 2008; Accepted May 7, 2008)

Abstract

Numerical investigations were performed with a supersonic inlet system installed with a three-dimensional bump which was substituted for a diverter or conventional ramp-type compression systems at Mach 2. The modified inlets were designed to have two oblique shocks and a terminal normal shock followed by a subsonic diffuser, with a circular cross-section throughout. A numerical analysis was conducted to understand the three-dimensional flow field including shock/boundary layer interactions that occur around a three-dimensional bump and to evaluate the performance of the supersonic inlets. The current numerical simulations showed a bump-type inlet based on a conventional ramp-type inlet can provide an improvement in total pressure recovery downstream of the shock/boundary-layer interaction over a ramp-type inlet.

Keywords: Supersonic inlet flow; Shock/boundary-layer interaction; Turbulent flow; Three-dimensional bump; Total pressure recovery

1. Introduction

A supersonic inlet has to provide homogeneous, low speed and high pressure air flow to the compressor face of an engine over a wide range of speeds, altitudes, and maneuvering conditions. Higher speed aircrafts generally require more complicated compression systems such as a series of movable compression ramps, porous walls, slots controlled by sophisticated software and complex mechanical systems [1]. In a high-speed supersonic aircraft configuration (e.g., $M_\infty=2\sim 5$), a compression system produces a series of oblique shock waves to reduce flow speed from freestream value, followed by a terminal normal shock wave. The interaction of a shock wave with a turbulent boundary layer yields large adverse pressure gradients causing rapid thickening and possible separation of the boundary layer. The resulting

shock/boundary layer interactions may lead to total pressure losses and distorted boundary layer profiles, and flow oscillations that can seriously degrade engine performance. Therefore, inlet designs of high speed aircraft must consider the removal of the boundary layer which contains low-energy air that flows near the wall surface of the fuselage and inlet at subsonic and supersonic speeds. A supersonic aircraft dealt with this boundary layer phenomenon by redirecting airflow such as a diverter of a gap between the fuselage and the upper lip of the inlet or the combinations of splitter plates and bleed systems [2]. The bleeding flow, which may remove the thick boundary layer from the inside of the diffuser, can consume a significant fraction of the ingested inlet mass flow, and the amount required increases as Mach number increases [3]. The bleeding mass flow reaches up to 15% of engine mass flow at Mach 2 which is proportional to the drag penalty. An aircraft eliminating the bleeding system, however, can reduce the empty weight reduction up to 12% [4].

*Corresponding author. Tel.: +82 53 810 2449, Fax.: +82 53 810 4627
E-mail address: djsong@yu.ac.kr
© KSME & Springer 2008

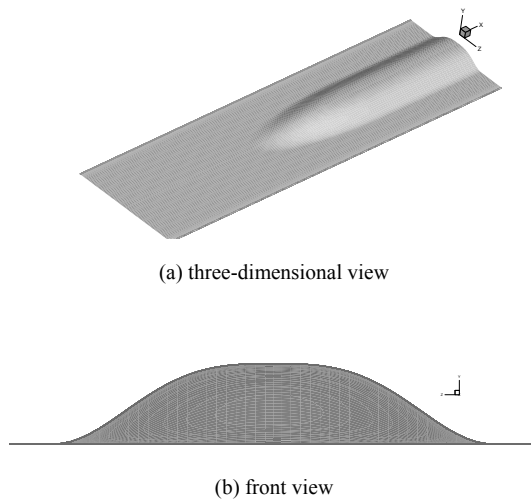


Fig. 1. Geometry of a three-dimensional bump.

The concept of three-dimensional surface to control the boundary layer in supersonic inlet flow has been investigated. Simon et al. studied an external bump-type inlet with boundary-layer bleeding, which yielded satisfactory operational stability over a range of Mach numbers from 1.5 to 2 [5]. A three-dimensional bump (Fig. 1) installed in the supersonic inlet may play a role as a compression surface and a removal system of boundary layers that prevents the low-energy airflow from entering the inlet instead of complex and heavy mechanical bleeding systems [2][6]. Therefore, it is of interest to study the effectiveness of compression systems using various bumps on shock/boundary-layer interactions in high-speed inlet flow.

2. Numerical method

2.1 Governing equation

The present three-dimensional computational analysis of fully turbulent supersonic inlet flow including oblique/normal shocks was carried out by using a numerical method [7] that integrates the governing equations on structured grids with a second-order upwind implicit scheme [8] for the convection terms of the conservation equations. The flow was modeled with the Reynolds-averaged Navier-Stokes equations for a thermally and calorically perfect gas, employing the Boussinesq hypothesis for turbulence modeling. The shear stress transport (SST) turbulence model was selected to close the Reynolds-averaged conservation equations because of its superior performance

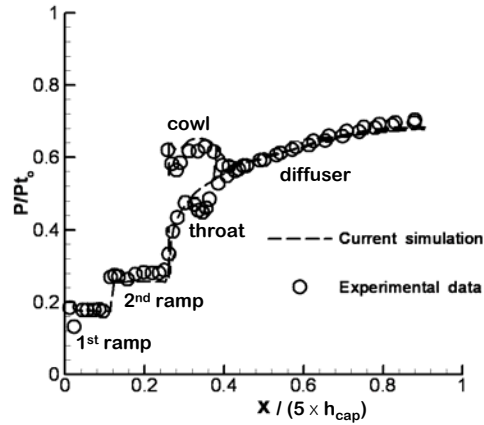


Fig. 2. Wall pressure distributions showing comparison of the current simulation with the experimental data of Loth et al. (2004) for a ramp-type inlet with a rectangular cross-section diffuser.

and stability as compared to other turbulence models for adverse pressure flows as shown in previous investigations [9][10]. The details of the conservation equations and the turbulence model are well documented in the above literature. Three-dimensional simulations with SST turbulence model were conducted to evaluate the validation of current numerical approach accessing the effect of the geometry variation on the primary performance measures. The static pressure distribution, which was non-dimensionalized by the inflow stagnation pressure, was plotted along the longitudinal wall surface in Fig. 2. Obvious sharp pressure increases were shown after the oblique and the normal shock waves in both the experiment and the current simulation. The pressure rise near the throat on the cowl surface was followed by a slight pressure-decrease region that resulted from the flow turning through the channel of the inlet throat. Downstream of the inlet throat, the gradual pressure rise approached the one of inviscid flow. This level of agreement in wall pressure distribution could put the confidence in resolving such as a current interaction problem between shock wave and boundary layer.

2.2 Grid system and boundary conditions

In this study on the flow characteristics around the bump in supersonic flow, a simple bump installed on the ramp with the cowl has a maximum height of $Y/D \approx 1$. In order to obtain solutions to the conservation equations, boundary conditions are required for the computational domain. At the inflow boundary of the

inlet flowfield without normal shock, the incoming flow properties were prescribed by the profiles obtained from the solution of a flat plate turbulent boundary layer flow. At the outflow boundary where the airflow exited the computational domain, the flow was mostly supersonic except for a small region near the wall, so that all flow variables were extrapolated. The back pressure was, however, specified at the outflow boundary in order to generate normal shock waves within the internal inlet flow field. The no-slip and adiabatic wall conditions were imposed on the wall surfaces. The grid system was composed of eight blocks in which each has over 4×10^5 mesh points. The viscous mesh had a first grid point from the wall at y^+ less than unity. A stretching function was used to cluster grid points near the wall and shock locations. Convergence of the solutions was considered to be achieved when the L^2 norm of the maximum residual reached 10^{-4} .

3. Result and discussion

3.1 The flow characteristics near the wall surface of a bump in a supersonic flow

A three-dimensional bump installed on the flat plate in supersonic flow field makes strong three-dimensional oblique shock waves around the bump leading edge and induces continuous increase of static pressure along the inclined surface of the bump. This oblique shock may form a three-dimensional shape resembling the bump geometry, and the airflow follows the curved surface of the bump, which fluid comes from the symmetric plane of the bump ($Z/D=0$) toward outside region of three-dimensional bump as shown in Fig. 3. This flow behavior occurs particularly near the wall surface of the bump where the flow energy is low and the flow speed is slow. Since the bump geometry eliminates low energy fluid from the thick boundary layer, it can reduce the thickness of boundary layer on the inclined wall surface of the bump and may keep sound boundary layer for adverse pressure gradient flow in the diffuser of a supersonic inlet.

Fig. 4 shows the contours of flow speed normalized by freestream sonic speed (A_∞) on the cross sections at four locations in the streamwise direction of a supersonic inlet flow. The thickness of boundary layer developed upstream of the bump (Fig. 4(a)) decreases rapidly (Fig. 4(b)), and becomes thinnest on the top of the bump (Fig. 4(c)). Even though the boundary layer

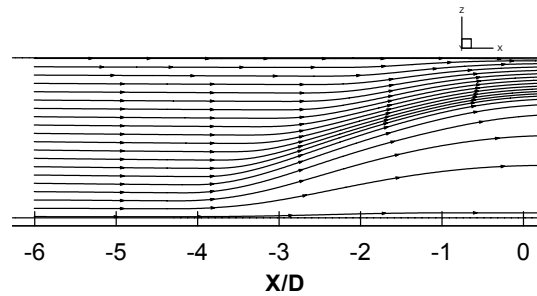


Fig. 3. Streamline around the leading edge of a three-dimensional bump.

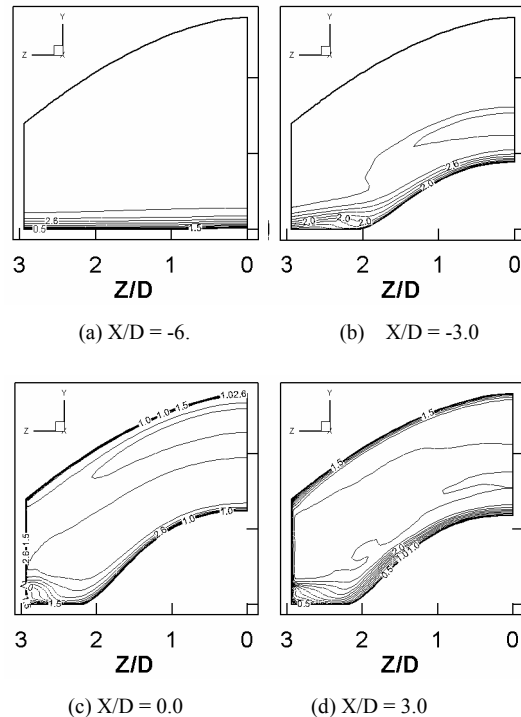


Fig. 4. Non-dimensional speed (V/A_∞) contours on the cross sections at four locations in streamwise direction for supersonic bump flow with a cowl at $M = 2.9$.

is interfered by the reflected shock, it maintains steadiness on the bump at this location as much as at the inlet boundary (Fig. 4(d)).

The total pressure distribution and development of boundary layer in supersonic inlet flow field are important in assessing the inlet performance because their loss and non-homogeneous distribution in internal flow degrades the engine performance and may severely reduce the lifetime of an aircraft. From this point of view, as shown above, a three-dimensional bump has potential advantages to control the internal

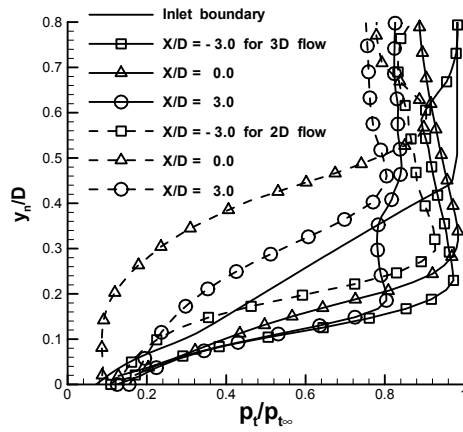


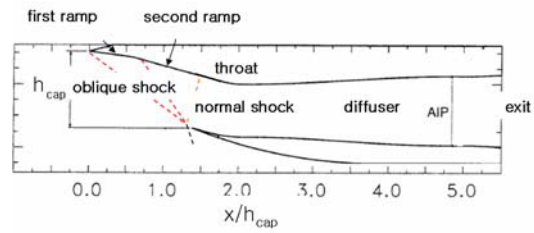
Fig. 5. Comparison of non-dimensional total pressure profiles between two and three-dimensional bump flows at $M = 2.9$.

flow for high-quality airflow in a supersonic inlet.

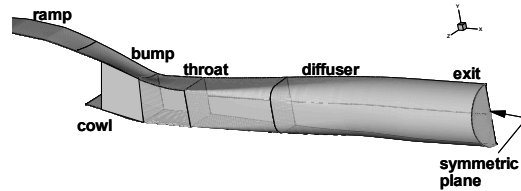
A two-dimensional bump was assumed to be same shape of a three-dimensional bump on the symmetric plane of the z -direction in order to scrutinize the flow characteristics and to understand the effect of the shape of the bump. As known, since two-dimensional flow may generate steeper angle and stronger oblique shocks than three-dimensional flow, it may induce the continuous development of the boundary layer on the inclined surface of a two-dimensional bump, which may yield a strong normal shock/boundary-layer interaction following reversed flow and sudden increase of the boundary-layer thickness. As shown in Fig. 5, the total pressure of two-dimensional bump flow was severely reduced near the wall surface after the reflected shock/boundary layer interaction at $X/D=3$. In three-dimensional bump flow, even though the shock loss was clearly shown over $y_w/D=0.4$, the defect of total pressure was reduced near the wall surface considerably as compared with the two-dimensional flow, which shows clearly the effect of a three-dimensional bump on the control of shock/boundary layer interaction.

3.2 The flow characteristics in a supersonic bump-type inlet

The original ramp-type inlet model was tested in the experiment of Loth et al. [11] which was conducted in the NASA Langley (LaRC) UPWT (Unitary Plan Wind Tunnel). The ramp-type inlet design was loosely based on an F-15 inlet (Fig. 6(a)), which had a low-expansion subsonic diffuser with a rectangular



(a) Schematic diagram of a conventional ramp-type inlet based on the experiment of Loth et al. (2004)



(b) Three-dimensional bump-type inlet

Fig. 6 The geometry of a supersonic ramp-type and bump-type inlets.

cross-section throughout. The cross-sectional area was then expanded only to lower Mach number to about 0.45 at the aerodynamic interface plane (AIP), which relied on the one-dimensional analysis of shock relationship and inviscid flow.

Fig. 6(b) shows the half geometry of a supersonic bump-type inlet in which flow field was assumed to be symmetric. This three-dimensional bump-type inlet consists of ramp, bump, throat, circular diffuser and cowl, which were based on a conventional ramp-type inlet of Loth et al. [11] and evolved to control shock/boundary-layer interactions effectively based on the previous study on three-dimensional bump. As shown in Fig. 6(b), the second ramp of the original ramp-type inlet was replaced by the three-dimensional bump. The ramp-type inlet of $h_o = 0$, however, adopted the original second ramp and the subsonic diffuser with a circular cross section throughout instead of the rectangular cross section in the experiment [11]. In the computation domain, the inlet boundary was freestream flow at Mach number of 2.0, and the static pressure of the outlet boundary was specified to stand the normal shock just in front of the cowl lip.

Fig. 7 shows the non-dimensional static pressure (p/p_∞) contours near the throat, which includes two oblique and a normal shocks on the symmetric plane of various bump-type inlets. It shows the severe interaction with a normal shock and boundary layer near

the upper wall surface of the case of $h_o = 0.0$ which is ramp-type inlet (Fig. 7(a)), but the case of $h_o = 0.75$ which height is higher about 75% than the ramp-type inlet produced the small region of the shock/boundary-layer interaction just upstream of the throat (Fig. 7(d)).

A conventional ramp-type inlet with the strong shock/boundary-layer interaction induces slow flow recovery near the throat and produces very thick boundary layer downstream in Fig. 8(a). The bleed system has to consume a significant fraction of inlet mass flow to remove this thick boundary. The bump-

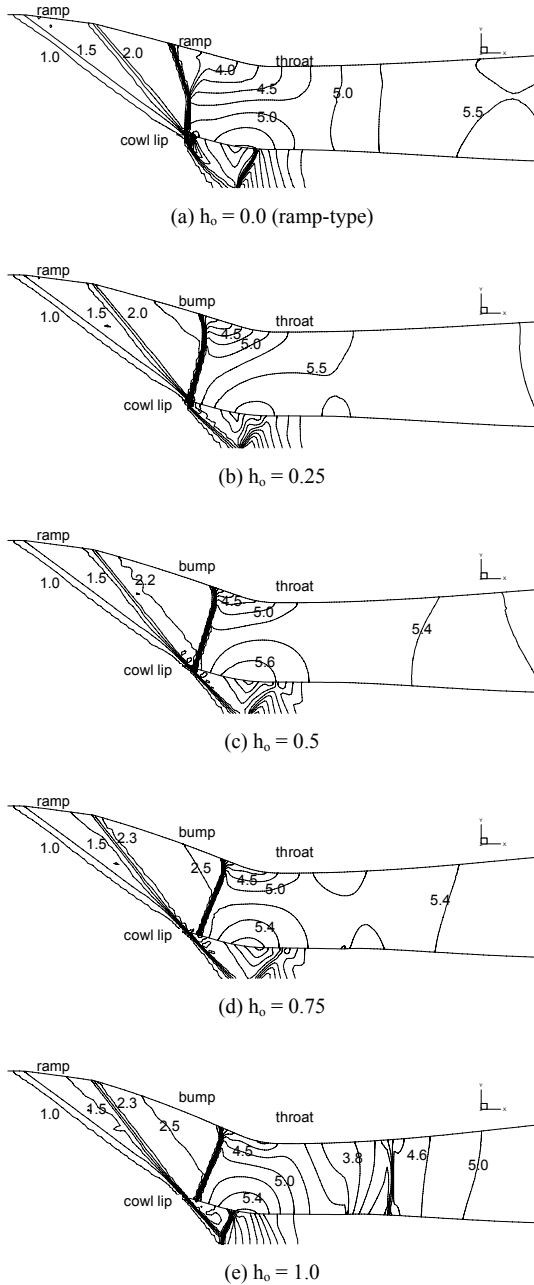


Fig. 7. Non-dimensional static pressure contours near the throat on the symmetric plane of various bump-type inlets at $M = 2.0$.

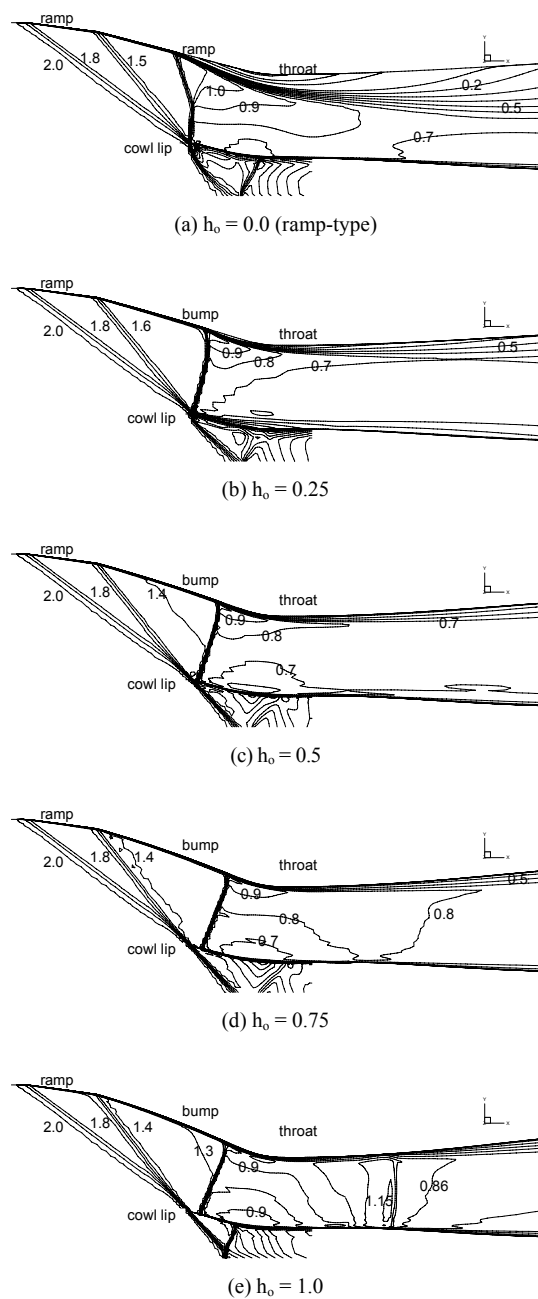


Fig. 8. Mach number contours near the throat on the symmetric plane of various bump-type inlets at $M = 2.0$.

type inlets (Figs. 8(b)~(d)), however, yielded that the flow field was rapidly recovered and retained sound boundary layer in the diffuser. The bump-type inlet may then eliminate the bleeding and the additional ducting systems, which can allow significant reduction of the weight for high speed vehicles [4][12].

Fig. 9 shows the comparison of total pressure contours at the AIP of the supersonic bump-type inlets. In particular, the shock/boundary-layer interaction can produce significant total pressure losses, boundary layer thickening and flow non-uniformities. Since the low energy fluid within boundary layer was removed effectively by the three-dimensional bump, a healthy boundary layer at the throat can produce the high total pressure recovery and uniform flow downstream. The bump-type inlet produced high recovery and wider uniform area of the total pressure as compared with the ramp-type inlet.

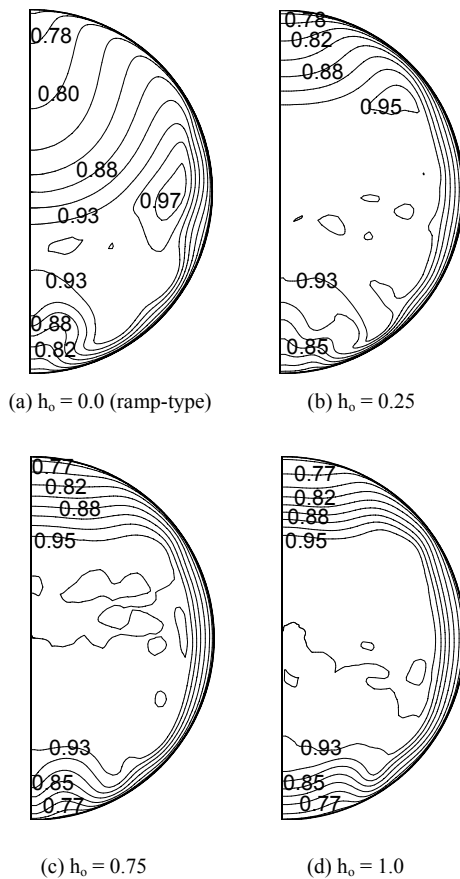


Fig. 9. Non-dimensional total pressure contours at the AIP showing comparison among a ramp-type inlet and three bump-type inlets at $M = 2.0$.

Fig. 10 shows the comparison of non-dimensional total pressure profiles on the symmetric plane among the experimental results [11], a ramp-type and various bump-type inlets. The results of the experiment and the current ramp-type inlet show that the total pressure profiles were severely distorted since the boundary layer was not recovered well under the adverse pressure gradient in the inlet diffuser. The total pressure profiles on the symmetric plane in bump-type inlets were, however, redeveloped rapidly, which can result in the high total pressure recovery and more uniformity.

Fig. 11(a) shows the change of the mass-weighted average total pressure (Π) at the AIP according to the variation of bump height. In these cases, the ramp-type inlet had the worst total pressure recovery of 0.89 (0.86 in the experiment of Loth et al. [11]). The case of $h_0 = 0.75$ shows the maximum value over other cases. The spatial flow-distortion (Δ) and standard deviation (Δ_d) indices were defined as

$$\Delta = \frac{(P_{t, \max} - P_{t, \min})}{P_{t, \text{avg}}} \quad \Delta_d = \sqrt{\frac{1}{m} \oint \left(\frac{P_t - P_{t, \text{avg}}}{P_{t, \infty}} \right)^2 dm} \quad (1)$$

Fig. 11(b) shows that the trend of two performance parameters is similar according to the change of the bump height. The case of $h_0 = 0.25$ shows the minimum values so that this case has the most uniform flow field among these cases studied herein. It shows that the bump-type inlet has limits of the bump height to produce better performance than the ramp-type inlet.

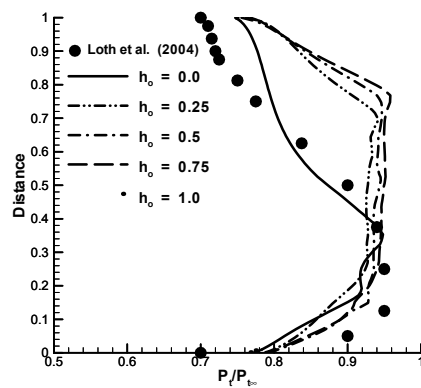
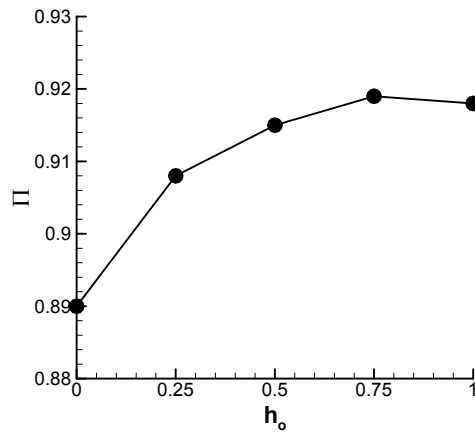
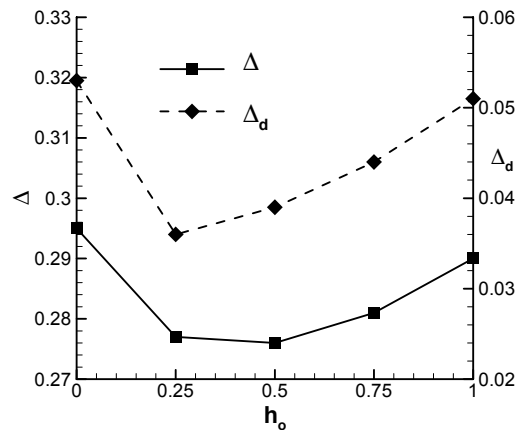


Fig. 10. Comparison of non-dimensional total pressure profiles on the symmetric plane among the experiment of Loth et al. (2004) and various bump-type inlets at the AIP at $M = 2.0$.



(a) Total recovery parameter (Π)



(b) Distortion (Δ) and standard deviation (Δₐ) indices

Fig. 11. Performance of various bump-type inlets at M = 2.0.

4. Conclusion

The current study simulated supersonic inlet flow with the shock/boundary layer interaction induced by a three-dimensional bump which was installed to substitute the ramp-compression system in a conventional supersonic inlet. This investigation, which was performed to elucidate the characteristics of the shock/boundary-layer interaction and the growth of turbulent boundary layer around a three-dimensional bump, shows the bump can play a critical role to reduce the total pressure loss and produce the healthy boundary layers downstream of the shock/boundary layer interaction. The bump-type inlet may have sound features for the inlet performance, which is able to produce an improvement of the total pressure recovery and flow uniformity downstream of the inlet

diffuser. Also, the height variation of the three-dimensional bump has some limitation to have optimum performance over the conventional ramp-type inlet. In the current study, the case of $h_0 = 0.75$ had the best performance in the total pressure recovery. In the future, however, more geometric parameters should be investigated to search the optimum design of a three-dimensional bump.

Acknowledgment

This work was supported by the Korea Research Foundation Grant funded by the Korea Government (MOEHRD) (No. R08-2004-000-10556-0) and the Yeungnam University research grants in 2007.

Nomenclature

A : Sonic speed
 D : Characteristic length
 D_o : Exit diameter of inlet diffuser
 M : Mach number
 p : Pressure
 V : Speed of flow
 X : Axis in a streamwise direction
 Y : Axis in a normal direction
 y_n : Normal distance from the wall surface
 Z : Axis in a spanwise direction

Subscripts

o : Stagnation property
 t : Total property
 ∞ : Freestream value

References

- [1] M. C. Gridley and S. H. Walker, Advanced Aero-Engine Concepts and Controls, AGARD Conf. Proc. 572, 86th Symposium, Seattle, WA, USA, (1996).
- [2] J. Seddon and E. L. Goldsmith, Intake Aerodynamics, Blackwell Science Ltd, (1999).
- [3] J. Benson and L. D. Miller, Mach 5 Turbo-Ramjet Inlet Design and Performance, ISABE 91-7079, ISABE Conference, Nottingham, U.K., 12 (1991) 746-753.
- [4] J. Anderson, Airframe/Propulsion Integration of Supersonic Vehicles, 26th AIAA/SAE/ASME/ASEE Joint Proportion Conference, AIAA 90-2151, Orlando, FL, USA, (1990).
- [5] P. C. Simon, D. W. Brown and R. G. Huff, Performance of External-Compression Bump Inlet at

- Mach Number of 1.5 to 2.0, NACA-RM-E56L19, National Advisory Committee for Aeronautics, Washington, USA (1957).
- [6] B. J. Tillotson, E. Loth and J. C. Dutton, Experimental Study of a Mach 3 Bump Compression Flowfield, 44th AIAA Aerospace Science Meeting and Exhibit, January 9-12, Reno, NV, USA, (2006).
- [7] S. D. Kim and D. J. Song, The Numerical Study on the Supersonic Inlet Flow Field with a Bump, *Journal of Computational Fluids Engineering*, 10 (3) (2005a) 19-26.
- [8] C. Hirsh, Numerical Computation of Internal and External Flows, JOHN WILEY & SONS, NY, USA, (1989) 493-594.
- [9] L. M. Nicolai, Fundamental of Aircraft Design, METS Inc. San Jose, CA, USA, (1975).
- [10] S. D. Kim, C. O. Kwon and D. J. Song, Comparison of Turbulence Models in Shock-Wave/Boundary-Layer Interaction, *KSME International Journal*, 18 (1) (2004) 153-166.
- [11] E. Loth, R. Jaiman, C. Dutton, S. White, F. Roos, J. Mace and D. Davis, Mesoflap and Bleed Flow Control for a Mach 2 Inlet, 42nd AIAA Aerospace Science Meeting, AIAA 2004-855, Reno, NV, USA, (2004).
- [12] E. Loth, Smart Mesoflaps for Control of Shock Boundary-Layer Interactions, AIAA Fluid Dynamics, AIAA 2000-2476, Denver, CO, USA, (2000).